Supporting information

Influence of power fluctuation on Ni-based electrode degradation and hydrogen evolution reaction performance in alkaline water splitting: Probing the effect of renewable energy on water electrolysis

Congying Liu[1], Bing Lin[1,*], Hailong Zhang[1], Yingying Wang[2], Hangzhou Wang[3], Junlei Tang[1,3,*] , Caineng Zou[1]

[1] School of Chemical and Chemical Engineering & Institute for Carbon Neutrality, Southwest Petroleum University, Chengdu 610500, China.

[2] Key Laboratory of Optoelectronic Chemical Materials and Devices (Ministry of Education), Jianghan University, Wuhan 430056, China.

[3] CNPC Shenzhen New Energy Research Institute Co., Ltd., Shenzhen 518000, China.

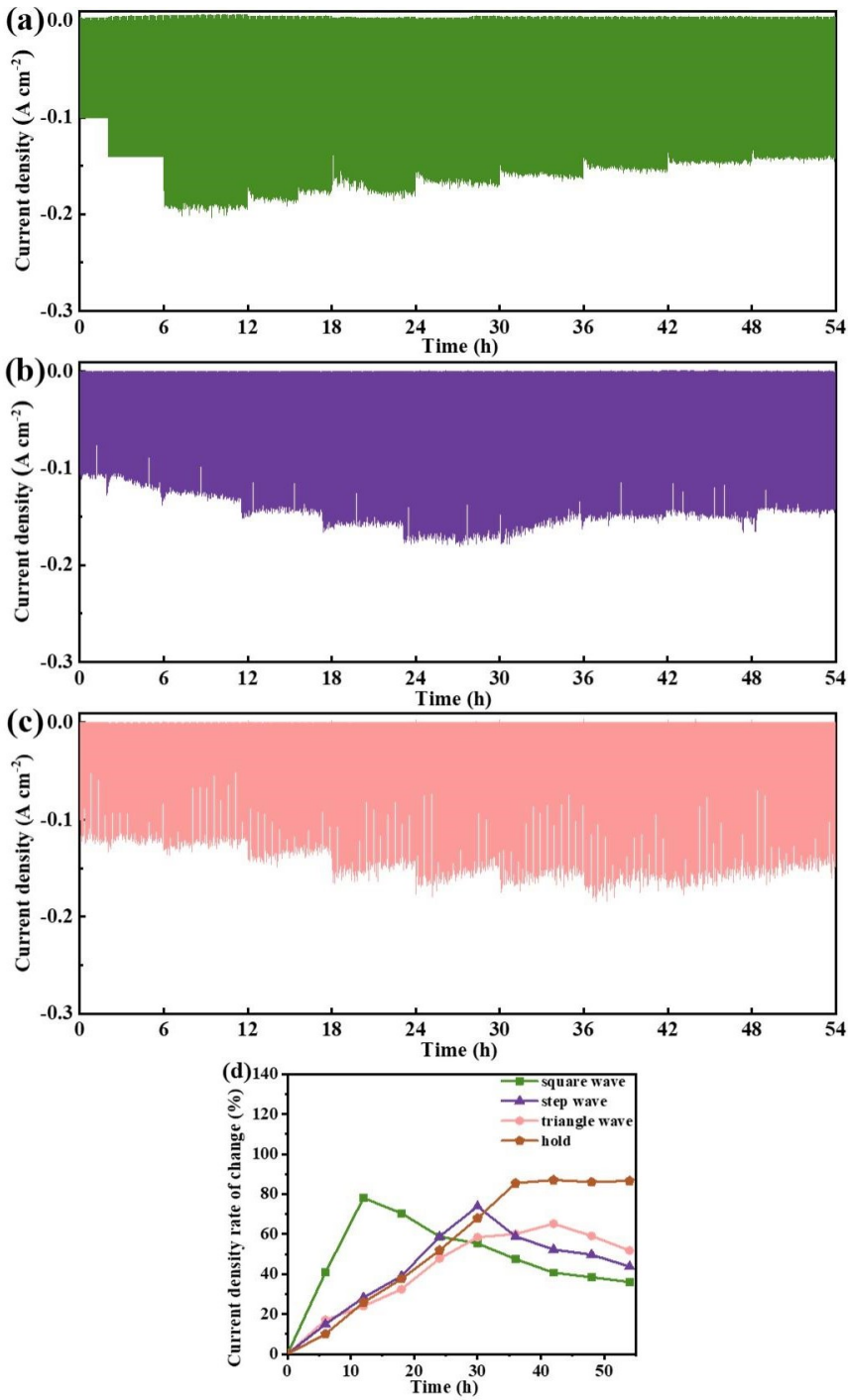

Fig. S1. T–I curves of plate Ni cathode in 1.0 mol L^{-1} NaOH solution at 80°C (a) Powered by square wave voltage. (b) Step wave. (c) Triangle wave. (d) The relationship between the current density change rate and time.

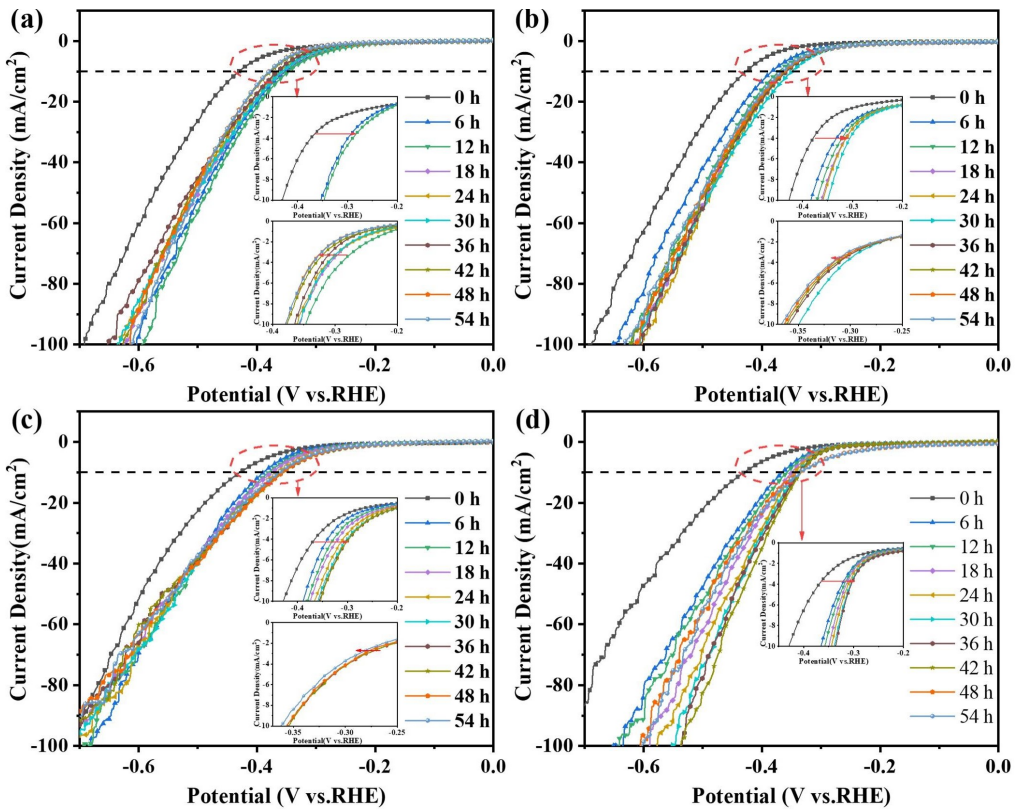

Fig. S2. LSV curves of the Ni cathode with fluctuation power. (a) Square wave. (b) Step wave. (c) Triangle wave. (d) Hold.

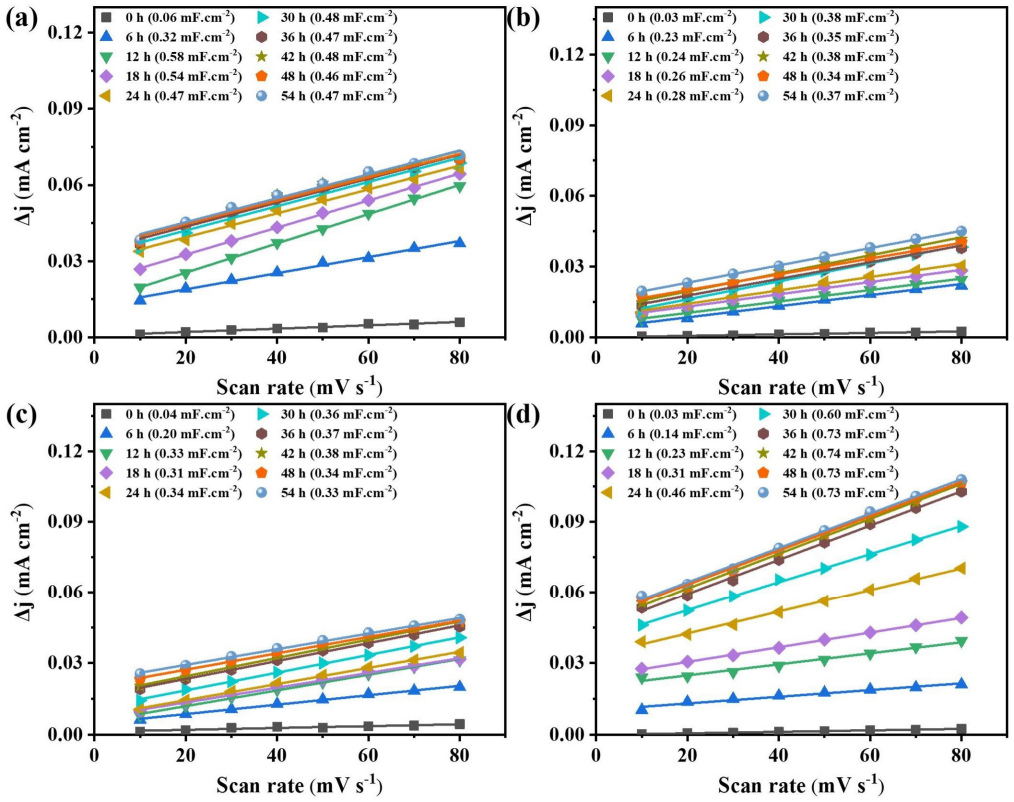

Fig. S3. Linear regression fitting was conducted to determine the C_{dl}. (a) Square wave. (b) Step wave. (c) Triangle wave. (d) Hold.

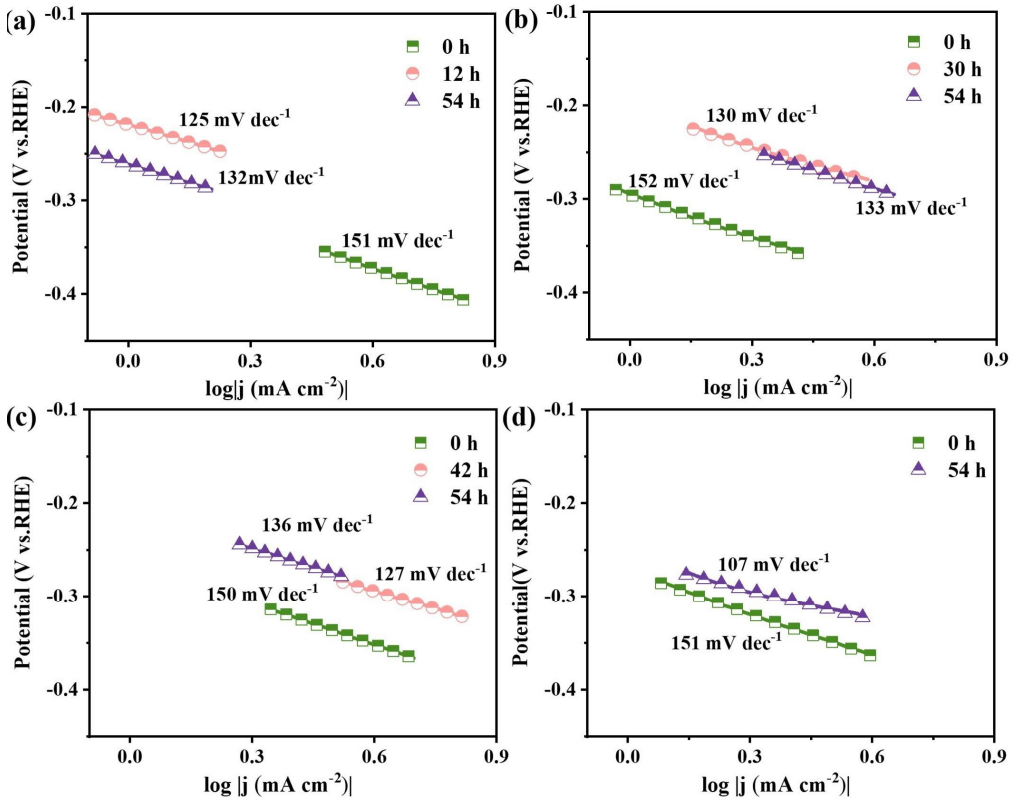

Fig. S4. The Tafel slope value at the pristine state, optimal performance and at the end of the test.

(a) Square wave. (b) Step wave. (c) Triangle wave. (d) Hold.

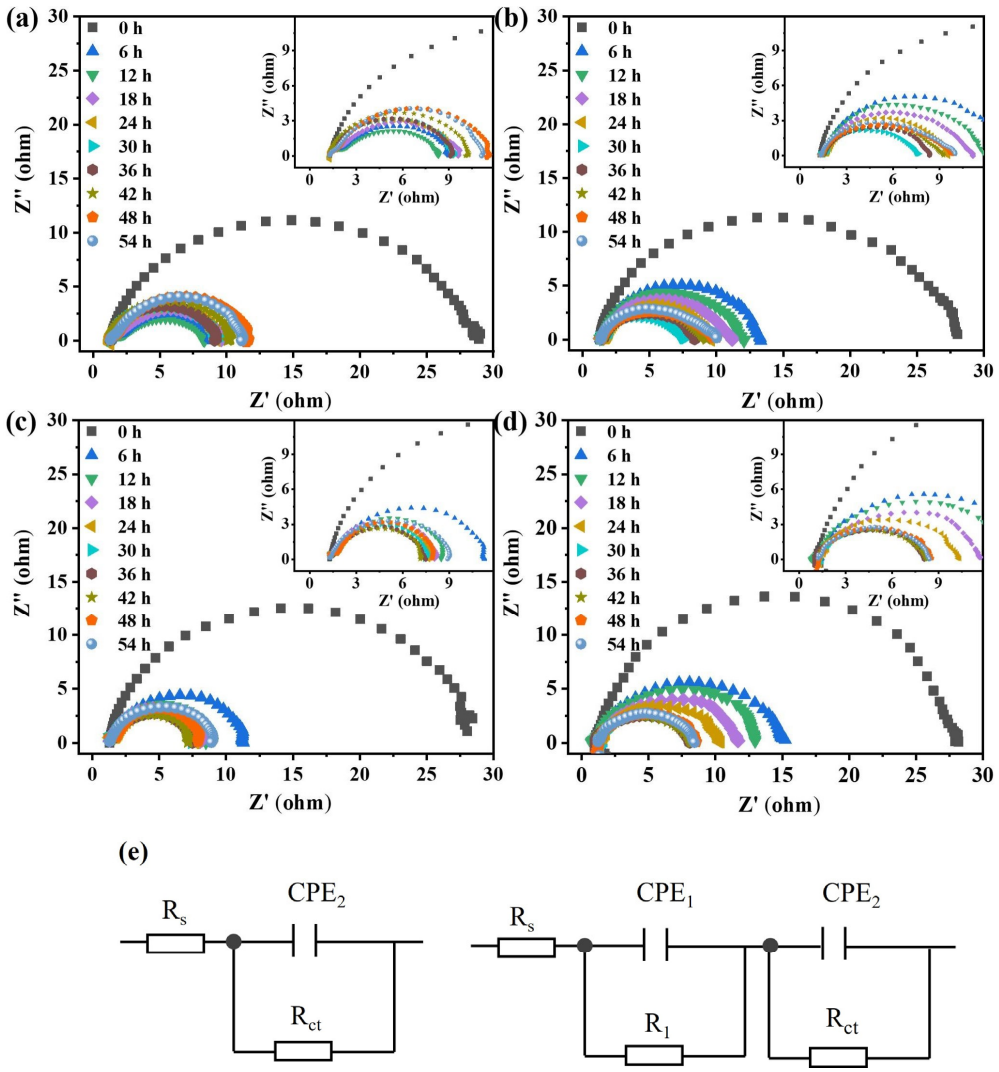

Fig. S5. Nyquist plots for EIS. (a) Square wave. (b) Step wave. (c) Triangle wave. (d) Hold.

(e) Equivalent electrical circuit diagramt.

Table S1. The variations of solution resistance (R_s), charge transfer resistance (R_{ct}) and R_1.

	Time/h	R_s/Ω	R_{ct}/Ω	R_1/Ω
Square wave	0	1.247	28.40	--
	12	1.267	6.30	0.85
	54	1.278	9.57	2.45
Step wave	0	1.270	26.47	--
	30	1.267	5.91	0.32
	54	1.277	6.33	1.51
Triangle wave	0	1.270	28.63	--
	42	1.273	5.54	0.37
	54	1.267	8.87	1.28
hold	0	1.263	26.39	--
	54	1.297	6.90	--

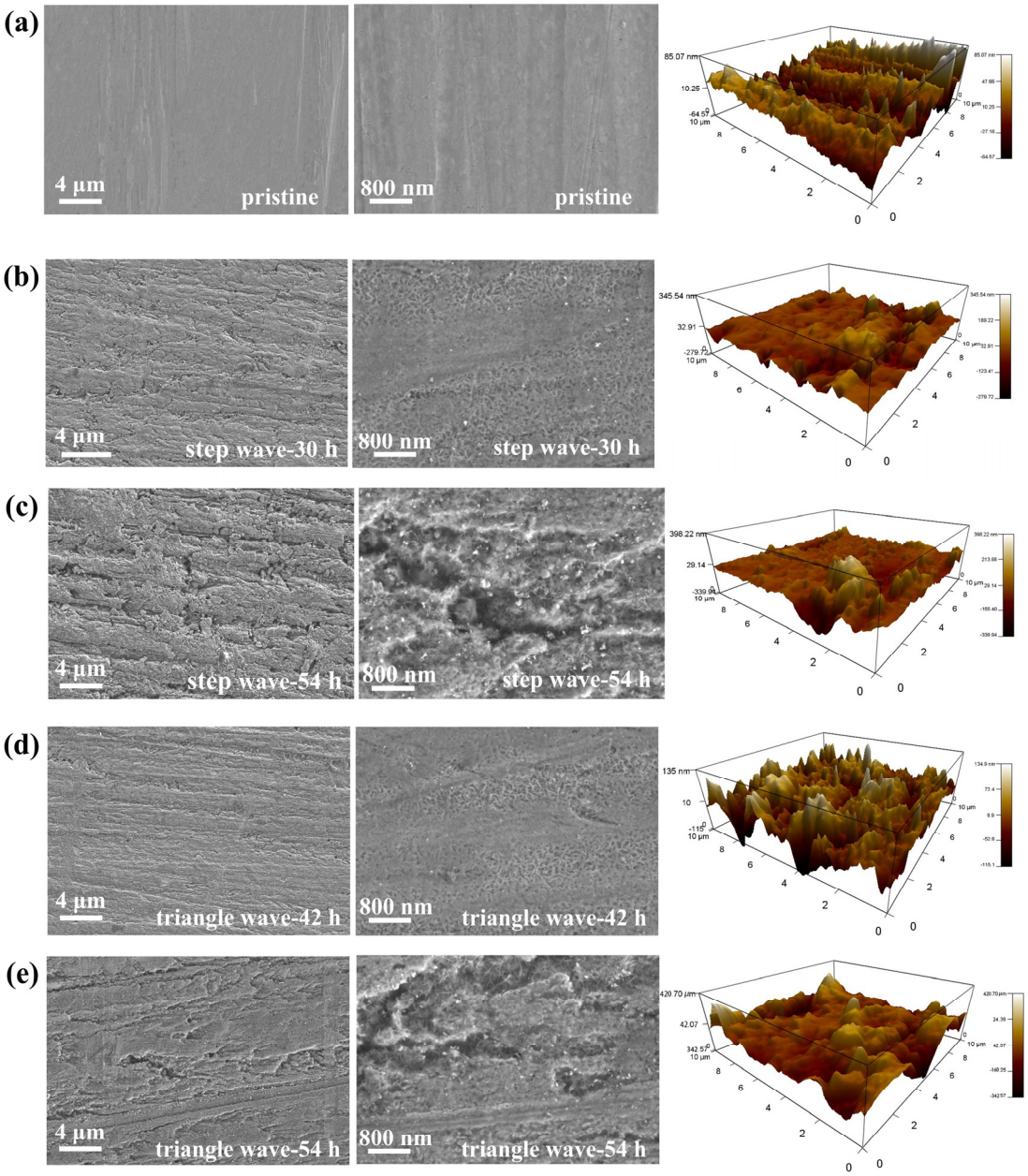

Fig. S6. SEM and AFM images of plate Ni cathode. (a) Pristine. (b) Optimal performance with step wave voltage. (c) End of test with step wave voltage. (d) Optimal performance with triangle wave voltage. (e) End of test with triangle wave voltage.

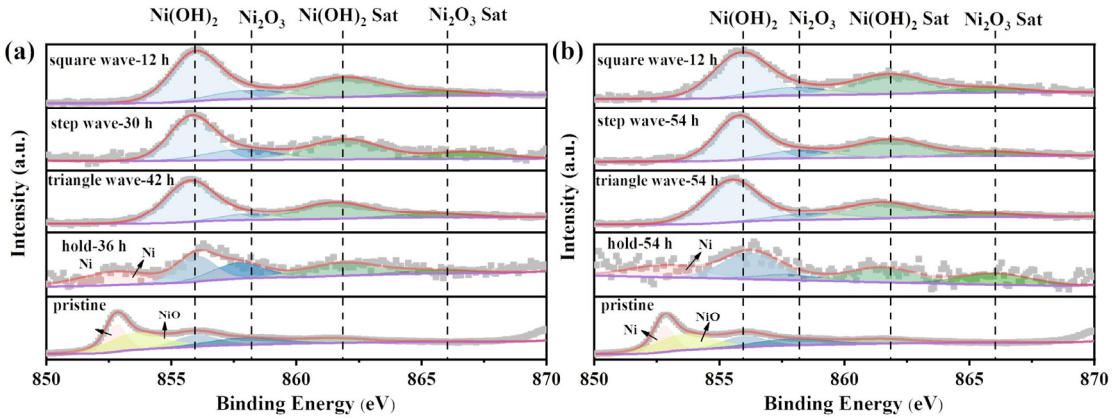

Fig. S7. XPS surface chemical analyses of plate Ni cathode. (a) Optimal performance. (b) End of the test.

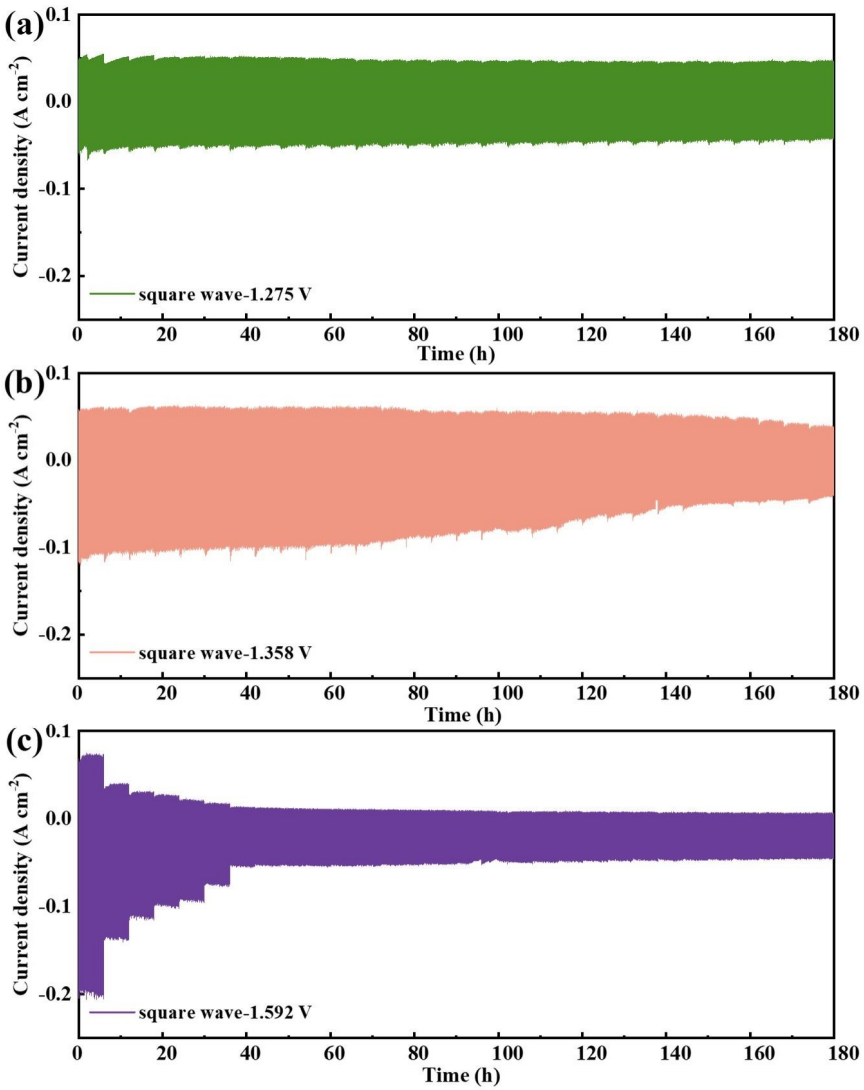

Fig. S8. T–I curves of FeNiMo-LDH@NiMo/SS for square wave test in 1.0 mol L^{-1} NaOH solution at 80°C. (a) -1.275~0 V. (b) -1.358~0 V. (c) -1.592~0 V.

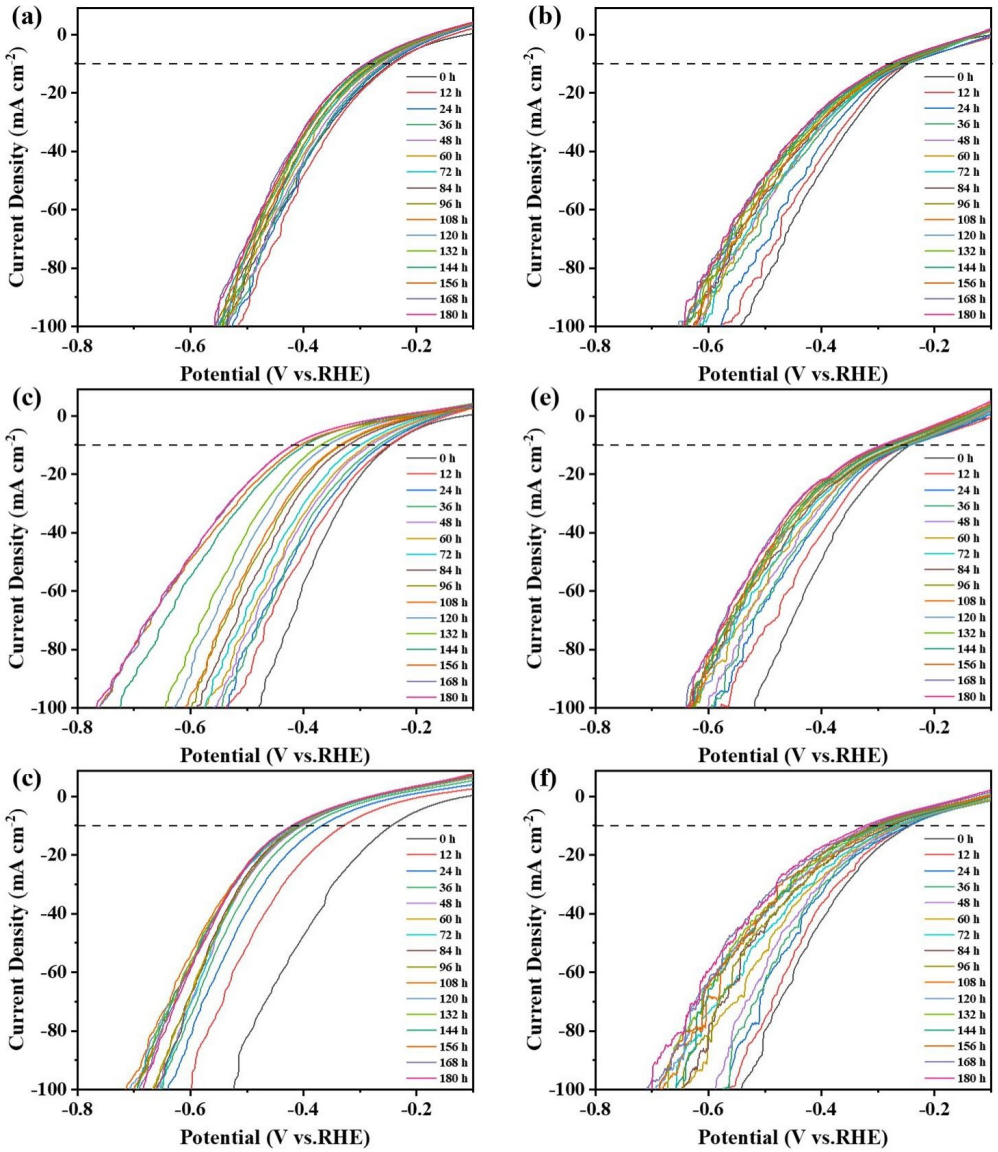

Fig. S9. LSV curves of FeNiMo-LDH@NiMo/SS. (a) -1.275~0 V in square wave. (b) -1.275 V in holding voltage. (c) -1.358~0 V in square wave. (d) -1.358 V in holding voltage. (e) -1.592~0 V in square wave. (f) -1.592 V in holding voltage.

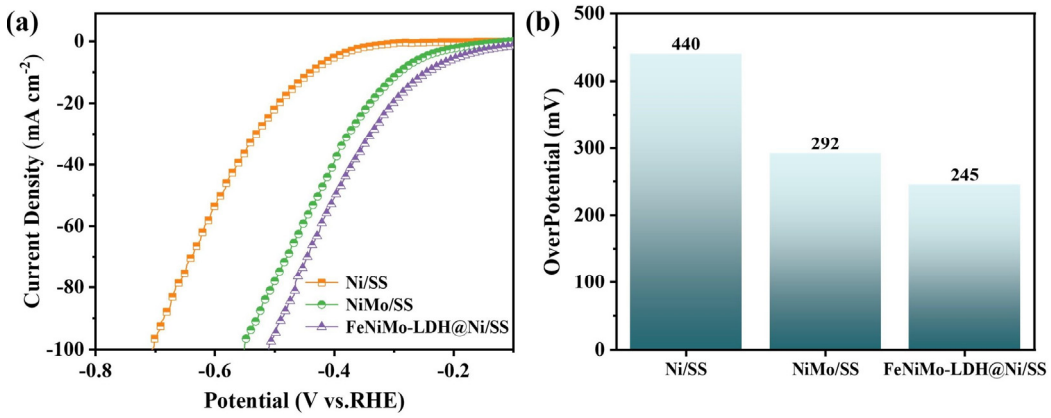

Fig. S10. Electrocatalytic HER performance of three catalytic electrodes. (a) LSV curves. (b) The overpotential at 10 mA cm^{-2}.

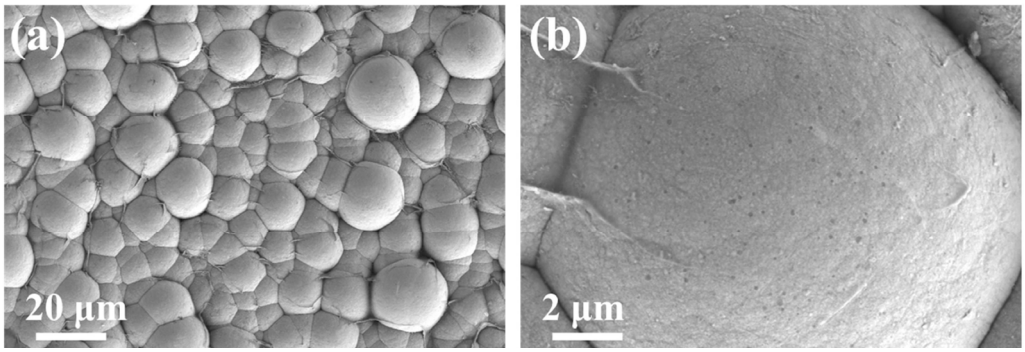

Fig.S11. SEM images of NiMo/SS. (a) 20 μm. (b) 2 μm.

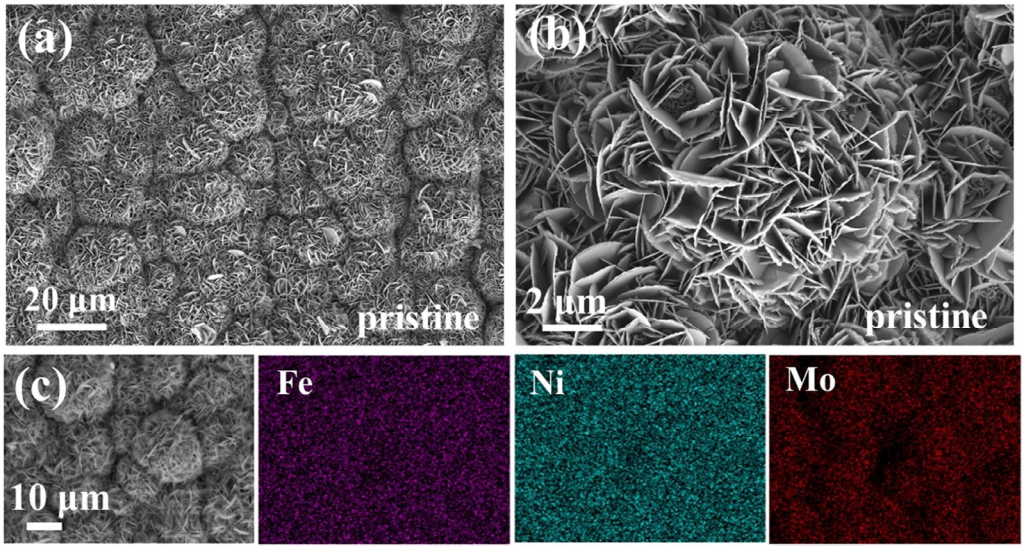

Fig.S12. SEM images of pristine FeNiMo-LDH@NiMo/SS. (a) 20 μm. (b) 2 μm.(c) EDS images of Fe, Ni and Mo.

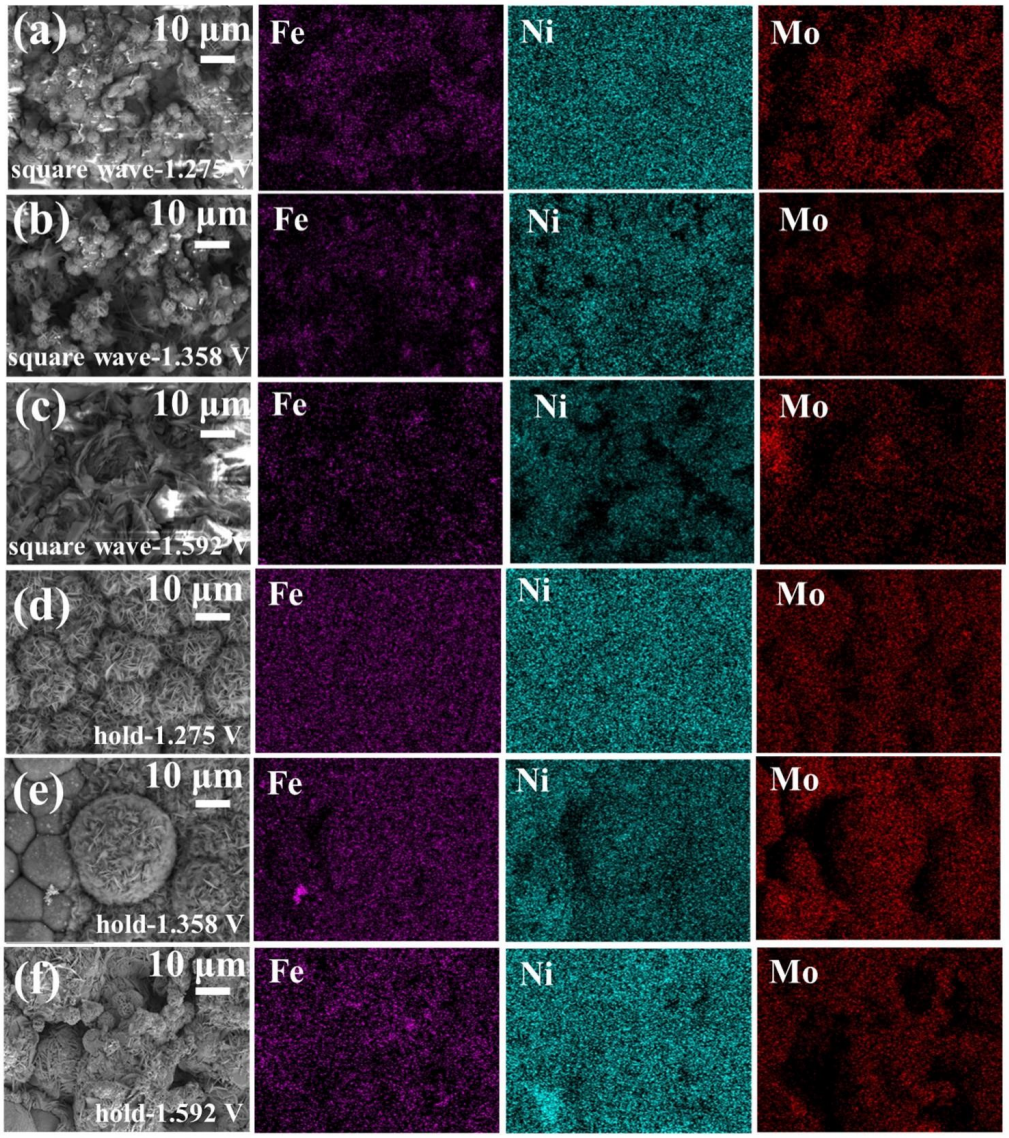

Fig.S13. EDS images of FeNiMo-LDH@NiMo/SS. (a) -1.275~0 V in square wave. (b) -1.358~0 V in square wave. (c) -1.592~0 V in square wave. (d) -1.275 V in holding voltage. (e) -1.358 V in holding voltage. (f) -1.592 V in holding voltage.

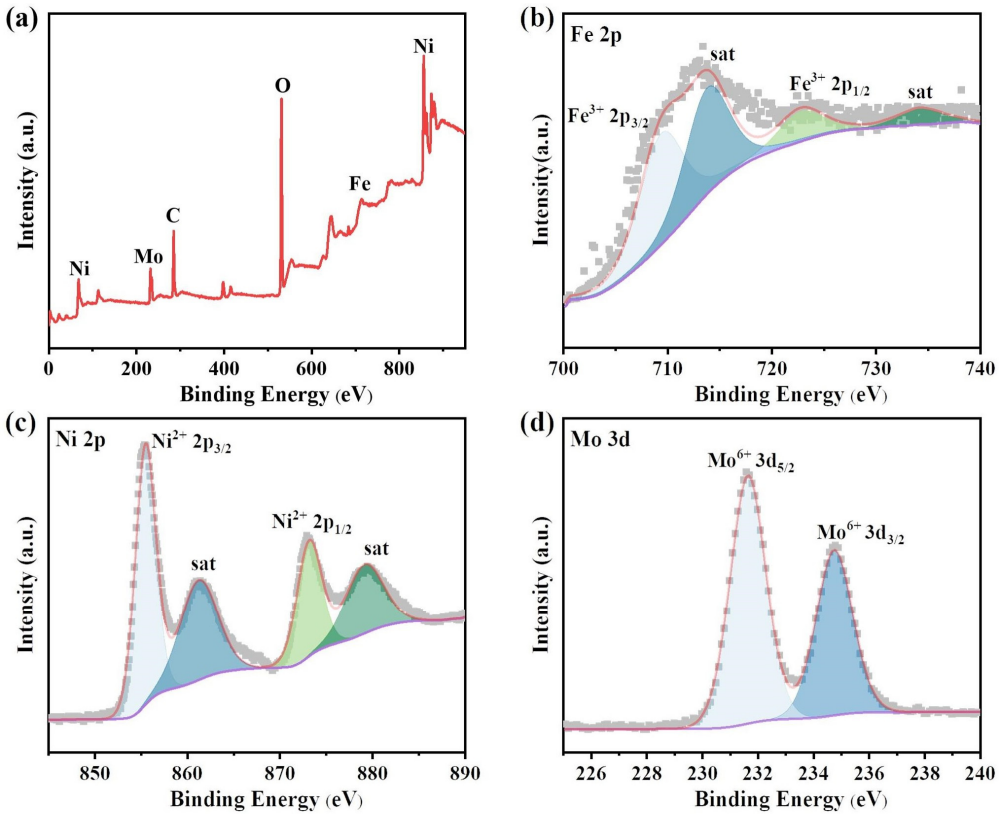

Fig. S14. XPS surface chemical analyses of pristine FeNiMo-LDH@NiMo/SS. (a) Wide-scan XPS spectra. (b) Fe 2p . (c) Ni 2p. (d) Mo 3d.

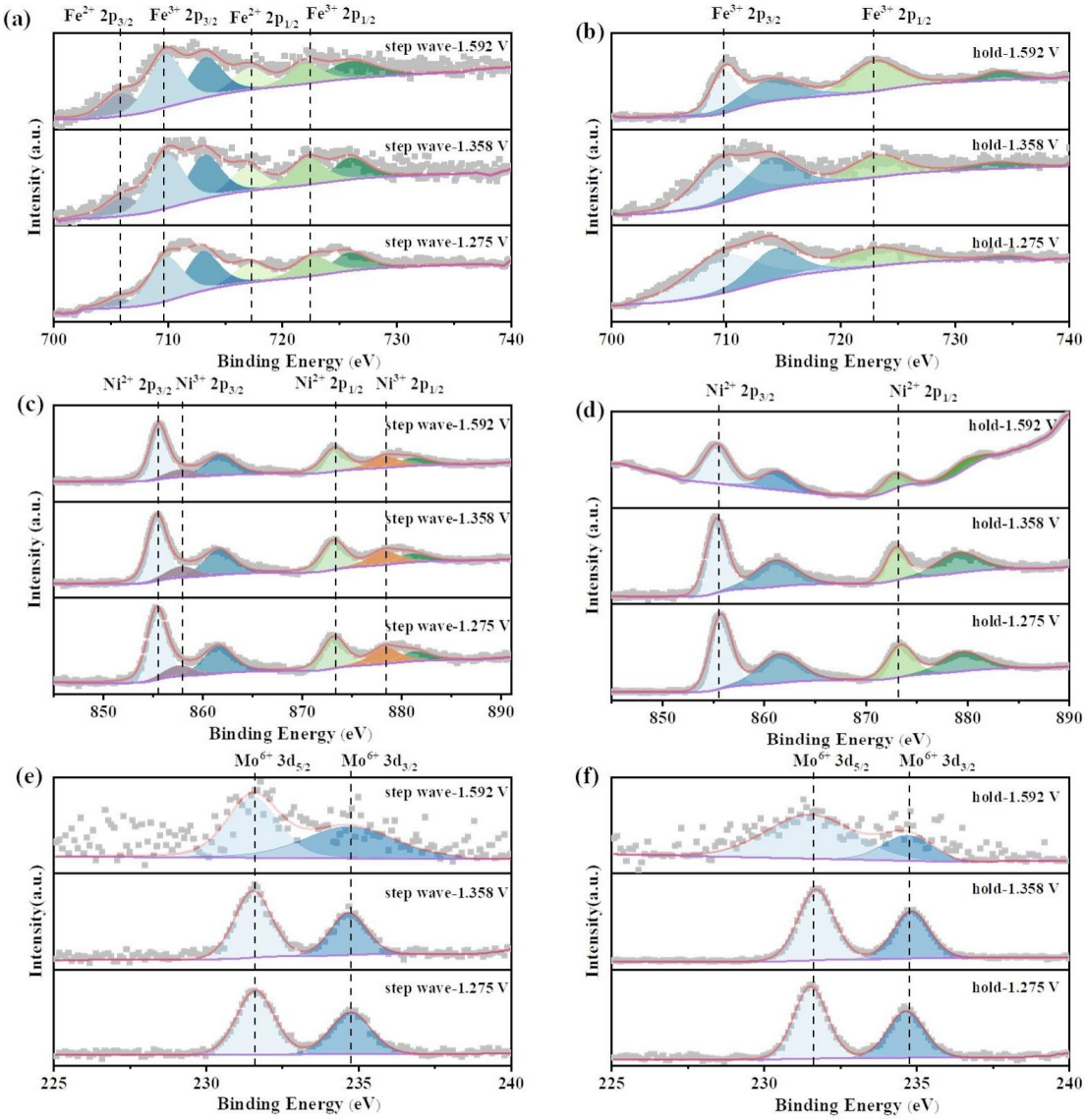

Fig. 15. XPS surface chemical analyses of FeNiMo-LDH@NiMo/SS. (a) Fe 2p in square wave. (b) Fe 2p in holding voltage. (c) Ni 2p in square wave. (d) Ni 2p in holding voltage. (e) Mo 3d in square wave. (f) Mo 3d in holding voltage.